Published in final edited form as:
J Nucl Med. 2013 August ; 54(8): . doi:10.2967/jnumed.112.118232.

Interaction of ^{11}C-Tariquidar and ^{11}C-Elacridar with P-glycoprotein and Breast Cancer Resistance Protein at the Human Blood-Brain Barrier

Martin Bauer[1], **Rudolf Karch**[2], **Markus Zeitlinger**[1], **Johann Stanek**[1,3], **Cécile Philippe**[1,4], **Wolfgang Wadsak**[4], **Markus Mitterhauser**[4], **Walter Jäger**[5], **Helmuth Haslacher**[6], **Markus Müller**[1], and **Oliver Langer**[1,3]

[1]Department of Clinical Pharmacology, Medical University of Vienna, Vienna, Austria

[2]Center for Medical Statistics, Informatics, and Intelligent Systems, Medical University of Vienna, Vienna, Austria

[3]Health and Environment Department, AIT Austrian Institute of Technology GmbH, Seibersdorf, Austria

[4]Department of Nuclear Medicine, Medical University of Vienna, Vienna, Austria

[5]Department of Clinical Pharmacy and Diagnostics, University of Vienna, Austria

[6]Department of Laboratory Medicine, Medical University of Vienna, Vienna, Austria

Abstract

The adenosine triphosphate-binding cassette transporters P-glycoprotein (Pgp) and breast cancer resistance protein (BCRP) are 2 major gatekeepers at the blood-brain barrier (BBB) which restrict brain distribution of several clinically used drugs. In this study we investigated the suitability of the radiolabeled Pgp/BCRP inhibitors ^{11}C-tariquidar and ^{11}C-elacridar to assess Pgp density in human brain with PET.

Methods—Healthy subjects underwent a first PET scan of 120 min duration with either ^{11}C-tariquidar (n = 6) or ^{11}C-elacridar (n = 5) followed by a second PET scan of 60 min duration with (R)-^{11}C-verapamil. During scan 1 (at 60 min after radiotracer injection) unlabeled tariquidar (3 mg/kg) was intravenously administered. Data was analyzed using 1-tissue 2-rate-constant (1T2K) and 2-tissue 4-rate-constant (2T4K) compartment models using either metabolite-corrected or uncorrected arterial input functions.

Results—Following injection of ^{11}C-tariquidar or ^{11}C-elacridar, brain PET signal corrected for radioactivity in vasculature was very low (~0.1 standardized uptake value) with slow washout. In response to tariquidar injection, a moderate, but statistically significant rise in brain PET signal was observed for ^{11}C-tariquidar (+27 ± 15%, P = 0.014, paired t-test) and ^{11}C-elacridar (+21 ± 15%, P = 0.014) without changes in plasma activity concentrations. Low levels of radiolabeled metabolites (<25%) were detected in plasma at time points up to 60 min after injection of ^{11}C-tariquidar or ^{11}C-elacridar. The 2T4K model provided better data fits than the 1T2K model. Model outcome parameters were similar when metabolite-corrected or uncorrected input functions were

For correspondence contact: Oliver Langer, Department of Clinical Pharmacology, Medical University of Vienna, Währinger-Gürtel 18-20, 1090 Vienna, Austria. Tel.: +43 1 40400 2981; Fax: +43 1 40400 2998. oliver.langer@meduniwien.ac.at.
First author: Martin Bauer, Resident in Clinical Pharmacology, Department of Clinical Pharmacology, Medical University of Vienna, Währinger-Gürtel 18-20, 1090 Vienna, Austria. Tel.: +43 1 40400 2981; Fax: +43 1 40400 2998. martin.m.bauer@meduniwien.ac.at

Europe PMC Funders Author Manuscripts

used. There was no significant correlation between distribution volumes (V_T) of ^{11}C-tariquidar or ^{11}C-elacridar and V_Ts of (*R*)-^{11}C-verapamil in different brain regions.

Conclusion—The *in vivo* behavior of ^{11}C-tariquidar and ^{11}C-elacridar was consistent with that of dual Pgp/BCRP substrates. Both tracers were unable to visualize cerebral Pgp density, which was most likely related to insufficiently high binding affinities in relation to the very low density of Pgp in human brain (~1.3 nM). Despite their inability to visualize Pgp density, ^{11}C-tariquidar and ^{11}C-elacridar may find use as a new class of radiotracers to study the interplay of Pgp and BCRP at the human BBB in limiting brain uptake of dual substrates.

Keywords

P-glycoprotein; breast cancer resistance protein; blood-brain barrier; ^{11}C-tariquidar; ^{11}C-elacridar

INTRODUCTION

The adenosine triphosphate (ATP)-binding cassette (ABC) transporters P-glycoprotein (Pgp) and breast cancer resistance protein (humans: BCRP; rodents: Bcrp) act together as a team of gatekeepers at the blood-brain barrier (BBB) at the level of the luminal (blood-facing) membrane of vascular endothelial cells to protect the brain from the accumulation of mostly lipophilic xeno- and endobiotics (1). Various clinically used drugs, most notably several members of the family of tyrosine kinase inhibitors for cancer treatment (e.g. gefitinib, imatinib, sorafenib), were shown to be dual substrates of Pgp and BCRP (1). It has been demonstrated that Pgp and BCRP form a cooperative drug efflux system at the BBB and that dual substrates only gain brain access when both transporters are genetically or chemically disrupted (2). Tariquidar and elacridar are potent third-generation inhibitors of Pgp, which were later discovered to also inhibit BCRP, albeit at higher concentrations than Pgp (3). Based on the assumption that tariquidar and elacridar would bind to Pgp without being transported (4), ^{11}C-tariquidar and ^{11}C-elacridar were developed as PET tracers to visualize Pgp expression levels at the BBB as opposed to substrates, like ^{11}C-verapamil or ^{11}C-*N*-desmethyl-loperamide, which visualize Pgp function (5). However, initial preclinical evaluation revealed that baseline brain uptake of ^{11}C-tariquidar and ^{11}C-elacridar was very low in rats or mice and significantly increased in Pgp/Bcrp combination knockout mice or after pretreatment of animals with unlabeled tariquidar or elacridar (6-9). This “substrate-like” *in vivo* behavior was subsequently confirmed *in vitro* by showing that both tariquidar and elacridar are avidly transported by Pgp and BCRP in nanomolar concentrations as used for PET (10, 11). On the other hand, PET experiments in a low and high Pgp expressing murine breast tumor graft model showed higher uptake of ^{11}C-tariquidar in Pgp overexpressing tumors, consistent with Pgp binding (12). Similarly, paired PET scans with ^{11}C-tariquidar or ^{11}C-elacridar and (*R*)-^{11}C-verapamil in naïve rats, with an intravenous (i.v.) administration of tariquidar (3 mg/kg) before the (*R*)-^{11}C-verapamil scan, revealed a significant negative correlation between regional brain distribution volumes (V_Ts) of ^{11}C-tariquidar or ^{11}C-elacridar and (*R*)-^{11}C-verapamil, which also pointed to Pgp-specific binding of ^{11}C-tariquidar and ^{11}C-elacridar (13). Such a paired-scan protocol could in theory be used to independently assess Pgp expression and Pgp function in one scan session.

The aim of this study was to investigate the suitability of ^{11}C-tariquidar and ^{11}C-elacridar to visualize cerebral Pgp density in healthy human subjects. In analogy to a previous preclinical study (13) we performed paired PET scans with ^{11}C-tariquidar or ^{11}C-elacridar and (*R*)-^{11}C-verapamil including a pharmacological challenge with tariquidar (3 mg/kg).

Europe PMC Funders Author Manuscripts

MATERIALS AND METHODS

Subjects

The study was conducted in accordance with the Declaration of Helsinki and its amendments, registered with EUDRACT (number 2010-020759-30), and approved by the Ethics Committee of the Medical University of Vienna. The study was conducted as a prospective, single center, randomized, phase I study. All subjects provided written informed consent and were confirmed to be healthy based on medical history, physical examination, routine laboratory tests, urine drug screening, electrocardiography and vital signs. Eleven healthy men (mean age: 34 ± 8 y, mean weight: 76 ± 10 kg) were randomly assigned to receive either a ^{11}C-tariquidar (n = 6) or a ^{11}C-elacridar (n = 5) PET scan followed by a (R)-^{11}C-verapamil PET scan (Fig. 1).

Radiotracer Synthesis

^{11}C-Tariquidar, ^{11}C-elacridar and (R)-^{11}C-verapamil were synthesized following previously published procedures (8, 9, 14) and formulated in 20 mL sterile 0.9% (w/v) aqueous saline solution/ethanol (9/1, v/v) (containing 1.4% (v/v) Tween-80 in the case of ^{11}C-tariquidar and ^{11}C-elacridar). Radiotracer solutions were sterilized by passage through sterile Millex-GV filters (0.22 μm) (Millipore, Bedford, MA, USA). Tween-80 was used as an excipient to prevent non-specific binding of radiotracers to filter membranes. Tween-80 has been reported to inhibit Pgp with a half-maximum inhibitory concentration of 24 μM (15). In a previous preclinical study we have administered Tween-80 at doses up to 0.3 mmol/kg and failed to observe a Pgp inhibitory effect at the BBB (16). Specific activities at the time of injection were 19 ± 7 GBq/μmol, 42 ± 20 GBq/μmol and 38 ± 18 GBq/μmol for ^{11}C-tariquidar (n = 6 batches), ^{11}C-elacridar (n = 5 batches) and (R)-^{11}C-verapamil (n = 10 batches), respectively. Radiochemical purity of all radiotracers was >98%.

PET Study Protocol

Subjects underwent a first PET scan of 120 min duration with either ^{11}C-tariquidar or ^{11}C-elacridar followed by a second PET scan of 60 min duration with (R)-^{11}C-verapamil, with an interval of 1 h between the 2 scans (see Fig. 1). During scan 1 (at 60 min after tracer injection) tariquidar (AzaTrius Pharmaceuticals Pvt Ltd, London, UK) was administered at a dose of 3 mg/kg body weight (3.6 μmol/kg) as an i.v. infusion over 30 min. For formulation of the infusion solution, a stock solution of 7.5 mg/mL of tariquidar free base in 20% ethanol/80% propylene glycol was diluted in aqueous dextrose solution (5%, w/v) to a final volume of 250 mL.

PET Scans

All PET scans were performed on a GE Advance scanner run in 3-dimensional mode (GE Medical Systems). For scan 1, either ^{11}C-tariquidar (5.0 ± 0.8 MBq/kg corresponding to 0.3 ± 0.1 nmol/kg unlabeled tariquidar and 1.2 ± 0.8 μmol/kg Tween-80) or ^{11}C-elacridar (5.0 ± 0.5 MBq/kg corresponding to 0.2 ± 0.1 nmol/kg unlabeled elacridar and 0.5 ± 0.2 μmol/kg Tween-80) was i.v. injected over 30 s and dynamic emission scans were acquired for 120 min in 26 frames of increasing duration from 15 s to 10 min. For scan 2, (R)-^{11}C-verapamil (5.1 ± 0.7 MBq/kg corresponding to 0.2 ± 0.1 nmol/kg unlabeled (R)-verapamil) was injected over 30 s and dynamic emission scans were acquired for 60 min in 20 frames of increasing duration from 15 s to 10 min. Prior to each radiotracer injection a 5-min transmission scan using two ^{68}Ge pin sources was recorded.

Safety Monitoring

All subjects were monitored for safety parameters heart rate and blood pressure until they were discharged from the study ward the morning after the PET scan. In addition, clinical laboratory blood and urine tests were performed. Adverse events were recorded continuously and the relationship to the study drugs was assessed.

Blood Analysis

To determine arterial input function of ^{11}C-tariquidar and ^{11}C-elacridar, blood samples (2 mL each) were manually drawn from the radial artery at 7-s intervals for the first 2 min, followed by samples at 3.5, 5 and 10 min (9 mL each), 20, 30, 40 and 60 min (18 mL each) and 75, 90, 105 and 120 min (9 mL each) after radiotracer injection. Aliquots of blood and plasma were measured for radioactivity in a gamma counter which was cross-calibrated with the PET camera. Plasma samples collected at 3.5, 5, 10, 20, 30, 40 and 60 min were analyzed for radiolabeled metabolites of ^{11}C-tariquidar and ^{11}C-elacridar using a previously developed solid-phase extraction (SPE) assay (8). In brief, plasma (2-4 mL) was diluted with water (2 mL), spiked with unlabeled elacridar or tariquidar (10 μL, 20 mg/mL in dimethylsulfoxide), acidified with 5 M aqueous hydrochloric acid (40 μL) and loaded on a Sep-Pak vac tC18 cartridge (Waters Corporation, Milford, MA, USA), which had been pre-activated with methanol (3 mL) and water (5 mL). The cartridge was first washed with water (5 mL) and then eluted with methanol (2 mL) followed by aqueous ammonium acetate buffer (0.2 M, pH 5.0, 1.5 mL). Radioactivity in all 3 fractions (plasma, water, methanol/buffer) was quantified in a gamma counter. Radioactivity in the plasma and water fractions contained polar radiolabeled metabolites whereas unchanged ^{11}C-tariquidar and ^{11}C-elacridar were recovered in the methanol/buffer fraction. Recoveries of ^{11}C-tariquidar and ^{11}C-elacridar from the methanol/buffer fraction of the SPE assay ranged from 91-94%. The methanol/buffer fractions from 10, 20, 30, 40 and 60 min samples were further analyzed for radiolabeled metabolites of ^{11}C-tariquidar and ^{11}C-elacridar by reversed-phase high-performance liquid chromatography (HPLC) using a binary gradient system (see Supplemental Fig. 2 for HPLC conditions). Plasma input functions of ^{11}C-tariquidar and ^{11}C-elacridar were constructed by multiplying total activity concentrations in whole blood (from 0-60 min) with the mean ratios of plasma to whole blood activity (determined from 3.5, 5, 10, 20, 30, 40 and 60 min blood samples) with or without correcting for the fraction of polar radiolabeled metabolites, as determined by SPE, and by subsequent linear interpolation of the activity data. Blood sampling, metabolite analysis and input function generation for the (*R*)-^{11}C-verapamil scan were performed as described previously (14, 17). In addition, 4 venous 4-mL blood samples were collected from each subject at the end of the tariquidar infusion, at the end of the first PET scan and at the beginning and end of the second PET scan to measure tariquidar plasma concentration levels using a previously described liquid chromatography–tandem mass spectrometry (LC-MS) assay (18).

Image Analysis

T1-weighted MR images, acquired with a Philips Achieva 3.0T scanner (Philips Medical Systems, Best, The Netherlands), and the corresponding PET data were processed with Analyze 8.0 (Biomedical Imaging Resource, Mayo Foundation, MN, USA) and SPM5 (Wellcome Department of Imaging Neuroscience, UCL, UK) software as described previously (14). By using the Hammersmith n30r83 3-dimensional maximum probability atlas of the human brain (19) a template of preset volumes of interest (VOIs) was applied to the PET images to extract time-activity curves (TACs) for the following 7 gray matter regions: whole brain, hippocampus, cerebellum, caudate nucleus, putamen, thalamus and gyrus precentralis. These regions were chosen based on a previous preclinical study (20). For comparison of TACs between individual subjects, radioactivity concentrations (kBq/

mL) were normalized to injected radiotracer amount and expressed as standardized uptake values (SUVs). TACs of total radioactivity in whole blood multiplied by individual fractions of blood volume in brain (V_b) derived from kinetic modeling (see next section) were used to correct brain TACs for radioactivity in the vascular compartment.

Kinetic Modeling

For ^{11}C-tariquidar and ^{11}C-elacridar, datasets from 0 to 60 min of scan 1 (*i.e.* before tariquidar administration) were used for analysis. Standard 1-tissue 2-rate-constant (1T2K) and 2-tissue 4-rate-constant (2T4K) compartment models were fitted to the time-activity data of each VOI using plasma input functions either uncorrected or corrected for radiolabeled metabolites of ^{11}C-tariquidar and ^{11}C-elacridar. Time delays of 1 s to 4 s were considered in the input functions to account for the differences in the time course of activity between the arterial catheter and the arterial capillaries in the brain. From the fits, rate constants K_1, k_2 (1T2K model) and K_1, k_2, k_3, k_4 (2T4K model), respectively, as well as blood volume fraction in brain V_b were estimated and the distribution volume (V_T) of the respective brain VOI was calculated. Fits were performed by a software developed in-house using the method of weighted nonlinear least squares as implemented in the Optimization Toolbox of MATLAB (Mathworks, Natick, MA, USA). The quality of the fits was judged by visual inspection of observed and predicted activities together with the pattern of the residuals, by the correlation between observed and predicted activities, and by estimating parameter uncertainties (standard errors) from the diagonal elements of the covariance matrix as obtained from the inverse of the corresponding Fisher information matrix. Model selection (1T2K *versus* 2T4K) was based on the Akaike information criterion (AIC) (21). For (*R*)-^{11}C-verapamil scans a 2T4K model with plasma input function corrected for polar radiolabeled metabolites was used (17). Model outcome parameters obtained with the software developed in-house were cross checked using the General Kinetic Modeling Tool in PMOD (version 2.6.1, PMOD group, Switzerland).

Analysis of *ABCG2* and *ABCB1* Single Nucleotide Polymorphisms

Venous blood (4 mL) was drawn during the screening examination from all study participants for assessment of common *ABCG2* and *ABCB1* single nucleotide polymorphisms (SNPs) using previously described procedures (22, 23). For *ABCG2*, the C421A variant (ABI TaqMan Genotyping Assay C__15854163_70; Applied Biosystems, Rotkreuz, Switzerland) and for *ABCB1* the C1236T, G2677T and C3435T SNPs were determined.

Statistical Analysis

Statistical analysis was performed using Prism 5.0 software (GraphPad Software, La Jolla, CA, USA). A value of *P* less than 0.05 was considered significant.

RESULTS

Five subjects underwent ^{11}C-tariquidar and (*R*)-^{11}C-verapamil PET scans and 1 subject underwent only a ^{11}C-tariquidar PET scan. One subject was excluded from data analysis due to technical problems with the generation of the input function of ^{11}C-tariquidar. Five further subjects underwent ^{11}C-elacridar and (*R*)-^{11}C-verapamil PET scans.

There were no adverse or clinically detectable pharmacological effects related to the radiotracers injected in any of the 11 subjects. Dysgeusia and orthostatic hypotonia occurred as adverse events in 4 and 2 subjects, respectively, and were most likely related to the infusion of unlabeled tariquidar.

After the injection of ^{11}C-tariquidar or ^{11}C-elacridar, brain PET signal was very low (~0.1 SUV) and distributed uniformly throughout the brain with the exception of intense focal uptake in the venous sinus and the choroid plexus (Fig. 2). TACs of ^{11}C-tariquidar or ^{11}C-elacridar in plasma and whole brain gray matter are shown in Figure 3. One study subject who was scanned with ^{11}C-elacridar (subject 10) showed 2-3 fold higher activity concentrations in plasma and 3-4 fold higher activity concentrations in brain (Supplemental Fig. 1) as compared with the other study subjects and was therefore not included in the mean TACs shown in Fig. 3. At 60 min after injection of ^{11}C-tariquidar or ^{11}C-elacridar, unlabeled tariquidar was administered as an i.v. infusion over 30 min and PET data acquisition continued for a further 60 min (see Fig. 1). In response to tariquidar infusion, there was a small but clearly visible rise in brain PET signal both for ^{11}C-tariquidar and ^{11}C-elacridar, whereas plasma activity concentrations were essentially unchanged (Fig. 3). Brain PET signal (SUV) of ^{11}C-tariquidar was increased on average by 27 ± 15% (P = 0.014, paired t-test) at the end of scan 1 as compared with a time point before tariquidar infusion (45 min), whereas PET signal of ^{11}C-elacridar was increased by 21 ± 15% (P = 0.014). Interestingly, subject 10 showed only a very weak response to tariquidar infusion (+4% increase in brain SUV, Supplemental Fig. 1). Plasma activity concentrations before and after tariquidar infusion were not significantly different for ^{11}C-tariquidar (P = 0.368, paired t-test) and ^{11}C-elacridar (P = 0.283). In Supplemental Table 1, tariquidar plasma concentration levels at 4 different time points after tariquidar infusion are given for individual subjects.

Radioactivity in plasma samples collected at time points between 3.5 and 60 min after injection was analyzed for radiolabeled metabolites of ^{11}C-tariquidar and ^{11}C-elacridar using a SPE/HPLC assay. At all studied time points the fraction of polar radiolabeled metabolites of ^{11}C-tariquidar and ^{11}C-elacridar in plasma was <0.25 (Fig. 4). Radio-HPLC analysis of methanol/buffer eluates from the SPE assay did not show any radioactive species other than unchanged parent compound (Supplemental Fig. 2). Plasma-to-whole blood ratios of total radioactivity over time were rather stable, i.e. 1.34 ± 0.08, 1.39 ± 0.12 and 1.36 ± 0.08 at 3.5, 30 and 60 min after injection of ^{11}C-tariquidar (n = 5) and 1.51 ± 0.10, 1.51 ± 0.12 and 1.48 ± 0.10 at the same time points after injection of ^{11}C-elacridar (n = 5).

Data was modeled using 1T2K and 2T4K models with plasma input functions either uncorrected (Table 1) or corrected (Supplemental Table 2) for radiolabeled metabolites. The 2T4K model provided better fits (*i.e.* lower AIC values) than the 1T2K model. Representative 2T4K model fits for whole brain are shown in Figure 5. K_4 values in the 2T4K model were low, pointing to partially irreversible behavior (Table 1). Outcome parameters were similar when metabolite-corrected or uncorrected input functions were used, which supported the notion that the influence of radiolabeled metabolites on radiotracer kinetics was negligible. V_T and K_1 values of subject 10 in whole brain were approximately 1.5 fold above average (2T4K: K_1: 0.007; V_T: 0.51), whereas other outcome parameters were within normal range.

Regional 2T4K model-derived V_Ts of ^{11}C-tariquidar and ^{11}C-elacridar are shown in Figure 6. There was no statistically significant correlation between V_Ts of ^{11}C-tariquidar or ^{11}C-elacridar and V_T s of (*R*)-^{11} C-verapamil in different brain regions (Fig. 7). All study participants were genotyped for common functional SNPs of *ABCG2* and *ABCB1* (Supplemental Table 3). Subject 10 was a homozygous carrier of the TTT haplotype (1236T, 2677T, 3435T) in the *ABCB1* gene, but carried the wild-type *ABCG2* C421A allele.

DISCUSSION

This study is to our knowledge the first to describe the brain distribution and pharmacokinetics of radiolabeled third-generation Pgp inhibitors in humans. We found that brain PET signal of ^{11}C-tariquidar and ^{11}C-elacridar, when administered in tracer doses, was very low (Fig. 2), which was consistent with previous *in vitro* and *in vivo* data suggesting that these substances are concentration-dependently transported by Pgp and BCRP at the BBB (6-11, 16).

In analogy to a recent human PET study with (*R*)-^{11}C-verapamil (17), we administered unlabeled tariquidar during the ^{11}C-tariquidar and ^{11}C-elacridar PET scans (Fig. 1). Administration of Pgp inhibitor *during* the PET scan has been shown to allow for detection of Pgp efflux transport of a radiotracer at the BBB (24). The employed tariquidar dose (3 mg/kg), when given at 1 h before start of the PET scan, corresponded to the half-maximum effect dose for inhibition of Pgp at the human BBB (18). Despite the fact that we used a higher tariquidar dose in this study than in the previous (*R*)-^{11}C-verapamil study (2 mg/kg), we observed a much less pronounced rise in brain PET signal of ^{11}C-tariquidar and ^{11}C-elacridar in response to tariquidar than for (*R*)-^{11}C-verapamil (Fig. 3). The most likely explanation for this different behavior could be that (*R*)-^{11}C-verapamil is only transported by Pgp at the human BBB whereas ^{11}C-tariquidar and ^{11}C-elacridar are dual Pgp/BCRP substrates. Even though tariquidar in pharmacological doses is a dual Pgp and BCRP inhibitor, preclinical data suggests that higher doses than the presently employed 3 mg/kg dose would be needed to inhibit BCRP (16). Therefore it can be assumed that while Pgp was at least half-maximally inhibited, BCRP was still fully functional during administration of 3 mg/kg tariquidar and that BCRP efflux may have effectively limited brain access of both radiotracers. This behavior is in fact completely in line with what would be expected from dual Pgp/BCRP substrates (2). It has now been documented in the literature for several dual Pgp/BCRP substrates that their brain uptake is only moderately increased in single transporter knockout mice, *i.e. Mdr1a/b*$^{(-/-)}$ *or Bcrp1*$^{(-/-)}$ mice, relative to wild-type mice, whereby disproportionally large increases are seen in combination knockout mice (*Mdr1a/b*$^{(-/-)}$*Bcrp1*$^{(-/-)}$) (1). This is because of a cooperative effect of both transporters in preventing brain distribution of dual substrates (1). In line with this, brain-to-blood ratios of ^{11}C-tariquidar were found to be 1.0 ± 0.1 in wild-type, 3.3 ± 0.4 in *Mdr1a/b*$^{(-/-)}$, 1.8 ± 0.1 in *Bcrp1*$^{(-/-)}$ and 14.4 ± 1.7 in *Mdr1a/b*$^{(-/-)}$*Bcrp1*$^{(-/-)}$ mice (9).

We used 1T2K and 2T4K models for analysis and found that the 2T4K model provided better data fits (Fig. 5, Table 1). Importantly, we observed only low levels of radiolabeled metabolites of ^{11}C-tariquidar and ^{11}C-elacridar in plasma during the time course of the PET scan (Fig. 4 and Supplemental Fig. 2), which obviates the need to correct plasma input functions for radiolabeled metabolites. This poses a significant advantage over (*R*)-^{11}C-verapamil, which is extensively metabolized and gives radiolabeled metabolites, which are partly taken up into brain and may thereby confound PET measurements with this radiotracer (25). K_1 values of ^{11}C-tariquidar and ^{11}C-elacridar were up to 10-fold lower than those of (*R*)-^{11}C-verapamil (Table 1) (17), which suggested that ^{11}C-tariquidar and ^{11}C-elacridar were more effectively effluxed at the BBB than (*R*)-^{11}C-verapamil. Washout of ^{11}C-tariquidar and ^{11}C-elacridar from brain was very slow (Fig. 3). The good fits obtained with the 2T4K model (Fig. 5) suggest the presence of a second, deep brain compartment, the physiological correlate of which may be intracellular trapping of radiotracer in lysosomes, as recently reported for tariquidar (26).

Interestingly, subject 10 had approximately 1.5-fold higher V_T and K_1 values of ^{11}C-elacridar than the other subjects. Genetic analysis revealed that this subject was a homozygous carrier of the TTT haplotype in the *ABCB1* gene, which has been associated in

some studies with decreased Pgp expression/function and altered pharmacokinetics of Pgp substrate drugs (27). Thus, it is tempting to speculate that increased brain distribution of ^{11}C-elacridar in subject 10 may have been caused by decreased Pgp function at the BBB, although this finding needs to be confirmed in a larger cohort.

The original intention of developing ^{11}C-tariquidar and ^{11}C-elacridar was to visualize Pgp expression levels in brain. To investigate any possible Pgp binding of ^{11}C-tariquidar and ^{11}C-elacridar at the BBB, we combined ^{11}C-tariquidar and ^{11}C-elacridar PET scans with (*R*)-^{11}C-verapamil scans, after administration of 3 mg/kg tariquidar. We have shown previously that performing (*R*)-^{11}C-verapamil PET scans after half-maximal inhibition of Pgp is more sensitive to map regional differences in cerebral Pgp function than baseline scans (20). This is because brain uptake of (*R*)-^{11}C-verapamil is relatively low in baseline scans, which may make it difficult to detect any further reduction in brain uptake due to regionally increased Pgp activity.

Moreover, half-maximal Pgp inhibition may increase the percentage of (*R*)-^{11}C-verapamil in brain relative to its radiolabeled metabolites which are not or to a lower extent transported by Pgp (25), thereby providing better sensitivity to study regional Pgp function in brain. If ^{11}C-tariquidar and ^{11}C-elacridar bind to Pgp and (*R*)-^{11}C-verapamil is effluxed by Pgp, brain uptake of ^{11}C-inhibitors and ^{11}C-substrates should in theory be inversely related, *i.e.* brain regions with high uptake of ^{11}C-inhibitor should show low uptake of ^{11}C-substrate and *vice versa*. Such a behavior has in fact been observed in a study in rats in which the same paired-scan protocol was employed as in the present study (13). Contrary to these preclinical results, we found no significant correlation between regional brain V_Ts of ^{11}C-tariquidar or ^{11}C-elacridar and (*R*)-^{11}C-verapamil (Fig. 7). This strongly suggests that other than at the rodent BBB, where ^{11}C-tariquidar and ^{11}C-elacridar appeared to be both effluxed by Pgp and also to bind to some extent to Pgp, possibly *via* distinct binding sites, the behavior of these probes at the human BBB is dominated by Pgp/BCRP efflux. A possible reason for this could be species-dependent differences in transporter expression levels at the human and rodent BBB. Shortly after we developed ^{11}C-elacridar and ^{11}C-tariquidar, data on absolute Pgp expression levels in isolated brain microvessels of various species, including humans, appeared in the literature (28). Using an LC/MS-based quantitative proteomics approach the expression of MDR1 in isolated human brain microvessels was found to be 2.3-fold lower than that of mdr1a in mouse brain microvessels (6.1 ± 1.7 *versus* 14.1 ± 2.1 fmol/μg protein) (28). A commonly used predictor for the magnitude of specific signal that can be obtained with a radioligand for imaging of a molecular target is the ratio of the concentration of target protein in whole brain (B_{max}) to the equilibrium dissociation constant (K_D) of the radioligand (29). B_{max}/K_D is also referred to as binding potential and should ideally be >5 to achieve measurable specific binding. To estimate the B_{max} of Pgp in whole brain one needs to know the density of brain capillary endothelial cells as a proportion of brain tissue. This is different from total brain capillary volume (~5%), which is much higher because it includes blood volume. Assuming a brain capillary endothelial cell volume of 0.2% of total brain volume (30) and a protein content of brain capillaries of 10%, the B_{max} of Pgp in human brain is 1.3 nM. Based on a K_D value for binding of ^{3}H-tariquidar to Chinese hamster ovary resistant cells of 5.1 nM (4), the binding potential is 0.26, which is clearly too low to visualize Pgp in human brain with ^{11}C-tariquidar. Another factor which might contribute to the inability of ^{11}C-tariquidar and ^{11}C-elacridar to visualize Pgp density in human brain could be that BCRP expression levels and BCRP/Pgp expression ratios are higher at the human than at the rodent BBB (BCRP expression (fmol/μg protein): humans: 8.14 ± 2.26, mouse: 4.41 ± 0.69; BCRP/Pgp expression ratio: humans: 1.3, mouse: 0.3) (28). Thus, a relatively higher contribution of BCRP efflux at the human than at the rodent BBB could further reduce any possible Pgp binding of ^{11}C-tariquidar and ^{11}C-elacridar at the human BBB. In contrast to the BBB, Pgp density in the previously investigated murine

tumor model may have been higher and BCRP density lower, which could explain, possibly in combination with the absence of tight junctions in tumor capillaries, why ^{11}C-tariquidar was able to visualize Pgp expression in the tumor model (12). More generally, the ability of ^{11}C-tariquidar and ^{11}C-elacridar to provide a Pgp-binding signal may be tissue-specific, depending on Pgp relative to BCRP expression levels. Following these considerations, an effective radioligand to visualize Pgp density in human brain should ideally possess an at least ten-fold higher Pgp binding affinity than tariquidar and not be transported by BCRP and Pgp.

Despite the inability of ^{11}C-tariquidar and ^{11}C-elacridar to visualize cerebral Pgp density, these probes may find use as an entirely new class of PET tracers (as opposed to Pgp-selective substrates like (*R*)-^{11}C-verapamil or ^{11}C-*N*-desmethyl-loperamide) to study the interplay of Pgp and BCRP at the human BBB in limiting brain uptake of dual substrates (16). This is important because several clinically used drugs (e.g. tyrosine kinase inhibitors) are dual substrates of Pgp and BCRP (1) and no dual Pgp/BCRP substrates are currently available for PET studies in humans. Thus ^{11}C-tariquidar or ^{11}C-elacridar could be used as generic probes to assess brain penetration of dual Pgp/BCRP substrates in healthy subjects or glioma patients under various conditions, for example after treatment with Pgp/BCRP inhibitors like elacridar or in subjects with functional SNPs in the *ABCG2* and/or *ABCB1* genes.

CONCLUSION

Brain PET signal of ^{11}C-tariquidar and ^{11}C-elacridar was found to be very low in humans and only moderately sensitive to a pharmacological challenge with unlabeled tariquidar, which was consistent with the behavior of dual Pgp/BCRP substrates. ^{11}C-Tariquidar and ^{11}C-elacridar were not able to visualize Pgp density in human brain, which highlights the considerable challenge in visualizing low density multidrug efflux transporters at the human BBB with PET and furthermore suggests that compounds with subnanomolar Pgp binding affinities, which are currently not available, may be needed to develop successful radioligands. Despite their inability to visualize Pgp density, ^{11}C-tariquidar and ^{11}C-elacridar may find future clinical use as an entirely new class of radiotracers to assess the interplay of Pgp and BCRP at the human BBB.

Supplementary Material

Refer to Web version on PubMed Central for supplementary material.

Acknowledgments

The authors wish to thank Georgios Karanikas and the staff of the PET center at the Department of Nuclear Medicine and research nurse Maria Weber for their support in carrying out this study, Elisabeth Ponweiser and Raute Sunder-Plassmann for analysis of *ABCB1* SNPs and Michaela Böhmdorfer for measurement of tariquidar plasma concentrations. Divya Maheshwari (AzaTrius Pharmaceuticals Pvt. Ltd.) is acknowledged for providing tariquidar for i.v. injection and Joseph W. Polli (GlaxoSmithKline, Inc.) for providing the Investigator's Brochure of elacridar. This study was supported by the European Community's Seventh Framework program (Grant 201380) and by the Austrian Science Fund (FWF) (Grant F 3513-B20).

Financial support: European Community's Seventh Framework program (Grant 201380) and Austrian Science Fund (FWF) (Grant F 3513-B20)

REFERENCES

1. Agarwal S, Hartz AM, Elmquist WF, Bauer B. Breast cancer resistance protein and P-glycoprotein in brain cancer: two gatekeepers team up. Curr Pharm Des. 2011; 17:2793–2802. [PubMed: 21827403]
2. Kodaira H, Kusuhara H, Ushiki J, Fuse E, Sugiyama Y. Kinetic analysis of the cooperation of P-glycoprotein (P-gp/Abcb1) and breast cancer resistance protein (Bcrp/Abcg2) in limiting the brain and testis penetration of erlotinib, flavopiridol, and mitoxantrone. J Pharmacol Exp Ther. 2010; 333:788–796. [PubMed: 20304939]
3. Szakács G, Paterson JK, Ludwig JA, Booth-Genthe C, Gottesman MM. Targeting multidrug resistance in cancer. Nat Rev Drug Discov. 2006; 5:219–234. [PubMed: 16518375]
4. Martin C, Berridge G, Mistry P, Higgins C, Charlton P, Callaghan R. The molecular interaction of the high affinity reversal agent XR9576 with P-glycoprotein. Br J Pharmacol. 1999; 128:403–411. [PubMed: 10510451]
5. Kannan P, John C, Zoghbi SS, et al. Imaging the function of P-glycoprotein with radiotracers: pharmacokinetics and in vivo applications. Clin Pharmacol Ther. 2009; 86:368–377. [PubMed: 19625998]
6. Kawamura K, Yamasaki T, Konno F, et al. Evaluation of limiting brain penetration related to P-glycoprotein and breast cancer resistance protein using [(11)C]GF120918 by PET in mice. Mol Imaging Biol. 2011; 13:152–160. [PubMed: 20379788]
7. Kawamura K, Konno F, Yui J, et al. Synthesis and evaluation of [(11)C]XR9576 to assess the function of drug efflux transporters using PET. Ann Nucl Med. 2010; 24:403–412. [PubMed: 20361276]
8. Dörner B, Kuntner C, Bankstahl JP, et al. Synthesis and small-animal positron emission tomography evaluation of [^{11}C]-elacridar as a radiotracer to assess the distribution of P-glycoprotein at the blood-brain barrier. J Med Chem. 2009; 52:6073–6082. [PubMed: 19711894]
9. Bauer F, Kuntner C, Bankstahl JP, et al. Synthesis and in vivo evaluation of [^{11}C]tariquidar, a positron emission tomography radiotracer based on a third-generation P-glycoprotein inhibitor. Bioorg Med Chem. 2010; 18:5489–5497. [PubMed: 20621487]
10. Bankstahl JP, Bankstahl M, Römermann K, et al. Tariquidar and elacridar are dose-dependently transported by P-glycoprotein and Bcrp at the blood-brain barrier: a small-animal PET and in-vitro study. Drug Metabol Dispos. 2013; 41:754–762. [PubMed: 23305710]
11. Kannan P, Telu S, Shukla S, et al. The “specific” P-glycoprotein inhibitor tariquidar is also a substrate and an inhibitor for breast cancer resistance protein (BCRP/ABCG2). ACS Chem Neurosci. 2011; 2:82–89. [PubMed: 22778859]
12. Wanek T, Kuntner C, Bankstahl JP, et al. A comparative small-animal PET evaluation of [^{11}C]tariquidar, [^{11}C]elacridar and (*R*)-[^{11}C]verapamil for detection of P-glycoprotein-expressing murine breast cancer. Eur J Nucl Med Mol Imaging. 2012; 39:149–159. [PubMed: 21983837]
13. Kuntner C, Bankstahl JP, Bankstahl M, et al. Assessing cerebral P-glycoprotein expression and function with PET by combined [^{11}C]inhibitor [^{11}C]substrate scans [abstract]. Neuroimage. 2010; 52(suppl 1):S116.
14. Langer O, Bauer M, Hammers A, et al. Pharmacoresistance in epilepsy: a pilot PET study with the P-glycoprotein substrate R-[^{11}C]verapamil. Epilepsia. 2007; 48:1774–1784. [PubMed: 17484754]
15. Wang SW, Monagle J, McNulty C, Putnam D, Chen H. Determination of P-glycoprotein inhibition by excipients and their combinations using an integrated high-throughput process. J Pharm Sci. 2004; 93:2755–2767. [PubMed: 15389668]
16. Wanek T, Kuntner C, Bankstahl JP, et al. A novel PET protocol for visualization of breast cancer resistance protein function at the blood-brain barrier. J Cereb Blood Flow Metab. 2012; 32:2002–2011. [PubMed: 22828996]
17. Wagner CC, Bauer M, Karch R, et al. A pilot study to assess the efficacy of tariquidar to inhibit P-glycoprotein at the human blood-brain barrier with (*R*)-^{11}C-verapamil and PET. J Nucl Med. 2009; 50:1954–1961. [PubMed: 19910428]

18. Bauer M, Zeitlinger M, Karch R, et al. Pgp-mediated interaction between (*R*)-[^{11}C]verapamil and tariquidar at the human blood-brain barrier: a comparison with rat data. Clin Pharmacol Ther. 2012; 91:227–233. [PubMed: 22166851]
19. Hammers A, Allom R, Koepp MJ, et al. Three-dimensional maximum probability atlas of the human brain, with particular reference to the temporal lobe. Hum Brain Mapp. 2003; 19:224–247. [PubMed: 12874777]
20. Bankstahl JP, Bankstahl M, Kuntner C, et al. A novel PET imaging protocol identifies seizure-induced regional overactivity of P-glycoprotein at the blood-brain barrier. J Neurosci. 2011; 31:8803–8811. [PubMed: 21677164]
21. Akaike H. An information criterion (AIC). Math Sci. 1976; 14:5–9.
22. Hui L, DelMonte T, Ranade K. Genotyping using the TaqMan assay. Curr Protoc Hum Genet. 2008 Chapter 2:Unit 2.10.
23. Sunder-Plassmann R, Rieger S, Endler G, Brunner M, Müller M, Mannhalter C. Simultaneous analysis of MDR1 C3435T, G2677T/A, and C1236T genotypes by multiplexed mutagenically separated PCR. Clin Chem Lab Med. 2005; 43:192–194. [PubMed: 15843215]
24. Syvänen S, Blomquist G, Sprycha M, et al. Duration and degree of cyclosporin induced P-glycoprotein inhibition in the rat blood-brain barrier can be studied with PET. Neuroimage. 2006; 32:1134–1141. [PubMed: 16857389]
25. Lubberink M, Luurtsema G, van Berckel BN, et al. Evaluation of tracer kinetic models for quantification of P-glycoprotein function using (R)-[^{11}C]verapamil and PET. J Cereb Blood Flow Metab. 2007; 27:424–433. [PubMed: 16757979]
26. Kannan P, Brimacombe KR, Kreisl WC, et al. Lysosomal trapping of a radiolabeled substrate of P-glycoprotein as a mechanism for signal amplification in PET. Proc Natl Acad Sci U S A. 2011; 108:2593–2598. [PubMed: 21262843]
27. Cascorbi I. Role of pharmacogenetics of ATP-binding cassette transporters in the pharmacokinetics of drugs. Pharmacol Ther. 2006; 112:457–473. [PubMed: 16766035]
28. Uchida Y, Ohtsuki S, Katsukura Y, et al. Quantitative targeted absolute proteomics of human blood-brain barrier transporters and receptors. J Neurochem. 2011; 117:333–345. [PubMed: 21291474]
29. Eckelman WC, Mathis CA. Targeting proteins in vivo: in vitro guidelines. Nucl Med Biol. 2006; 33:161–164. [PubMed: 16546669]
30. Pardridge WM. Blood-brain barrier biology and methodology. J Neurovirol. 1999; 5:556–569. [PubMed: 10602397]

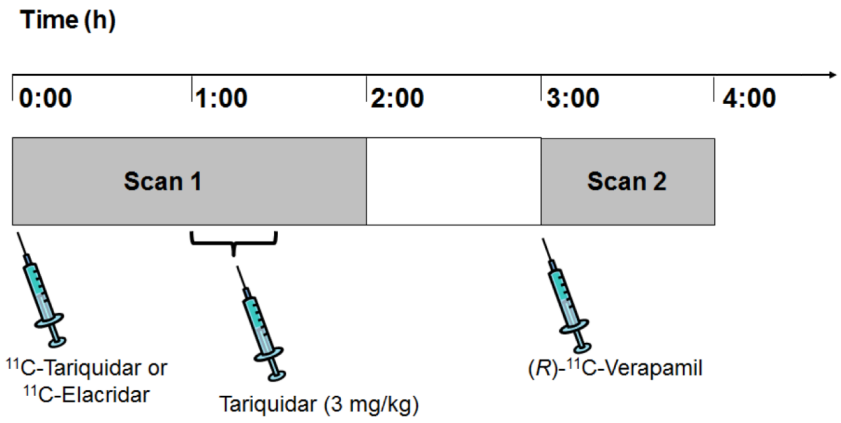

FIGURE 1.

Diagram of study set-up. PET scan 1 with either ^{11}C-tariquidar or ^{11}C-elacridar over 120 min was followed by PET scan 2 with (*R*)-^{11}C-verapamil over 60 min with an interval of 60 min between the 2 scans. At 60 min after start of scan 1, unlabeled tariquidar was infused i.v. at a dose of 3 mg/kg over 30 min.

Europe PMC Funders Author Manuscripts

Europe PMC Funders Author Manuscripts

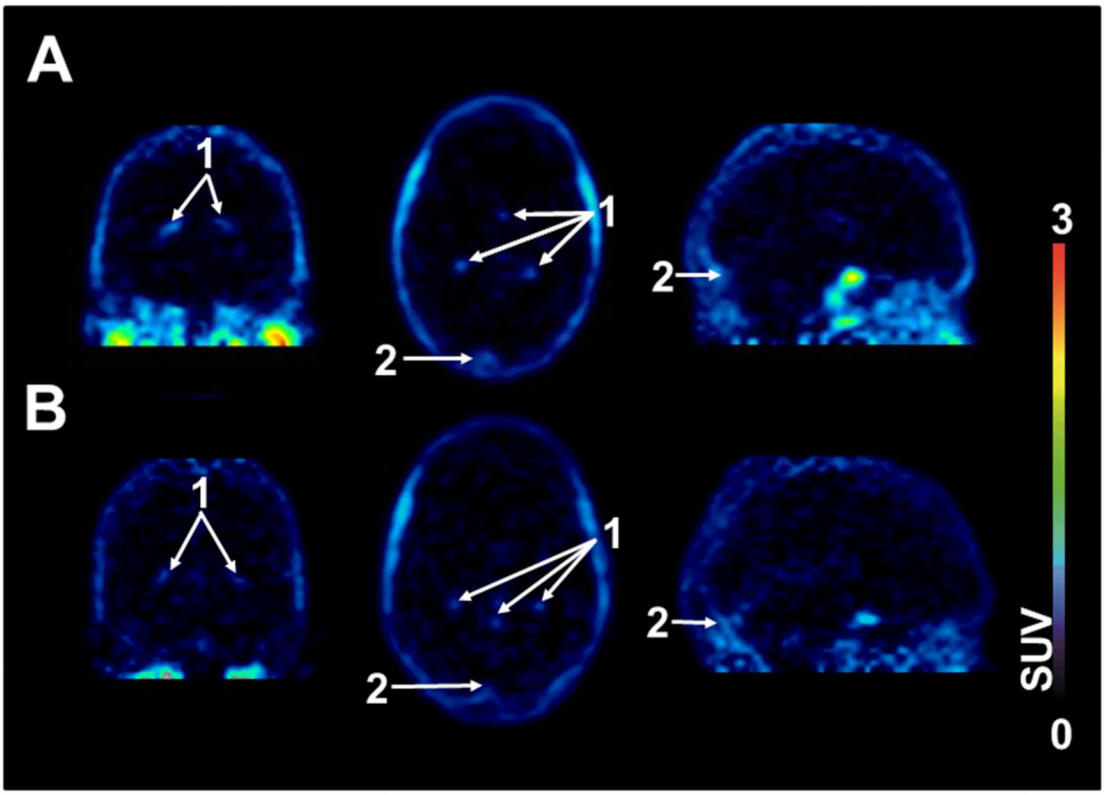

FIGURE 2.

Representative PET summation images (0-60 min) of ^{11}C-tariquidar (A) and ^{11}C-elacridar (B) in coronal (left), transaxial (middle) and sagittal views (right). Activity concentration is expressed as SUV and the radiation scale is set from 0 to 3. Anatomical structures are labeled using white arrows (1, choroid plexus; 2, venous sinus).

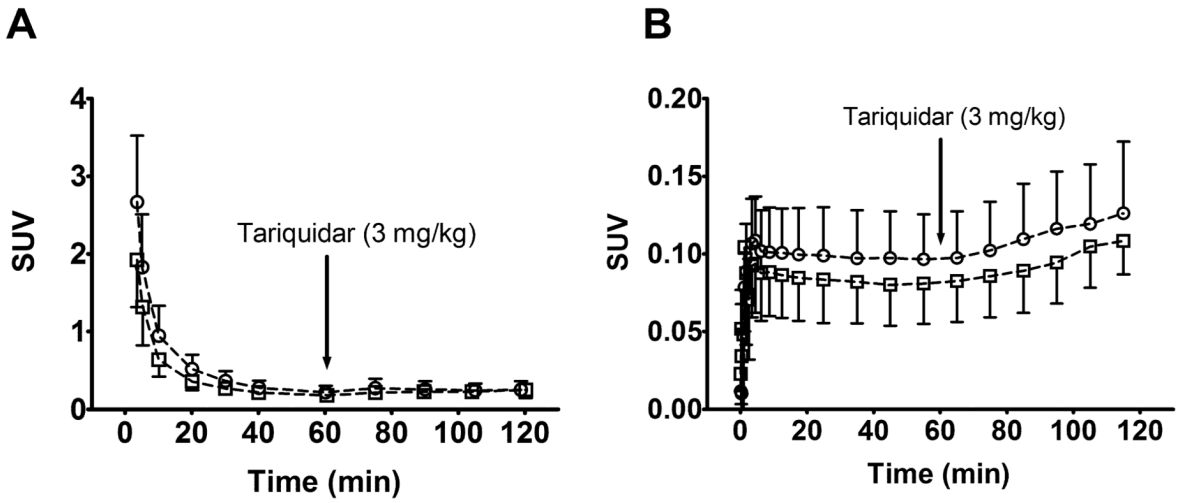

FIGURE 3.

Time-activity curves (mean SUV ± SD) of ^{11}C-tariquidar (open squares, n = 5) and ^{11}C-elacridar (open circles, n = 4, subject 10 not included) in arterial plasma, uncorrected for radiolabeled metabolites (A), and in whole brain gray matter, corrected for radioactivity in vasculature (B). The start of i.v. tariquidar infusion (3 mg/kg, over 30 min) is indicated by an arrow.

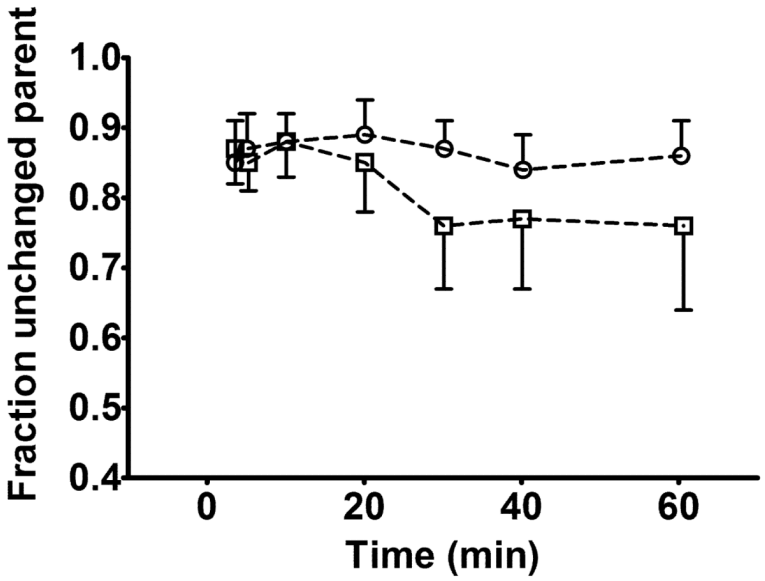

FIGURE 4.

Fractions (mean ± SD) of unchanged ^{11}C-tariquidar (open squares, n = 5) and ^{11}C-elacridar (open circles, n= 5) in arterial plasma over time as determined by solid-phase extraction assay. The shown values are not corrected for recoveries of ^{11}C-tariquidar and ^{11}C-elacridar, which ranged from 91-94%.

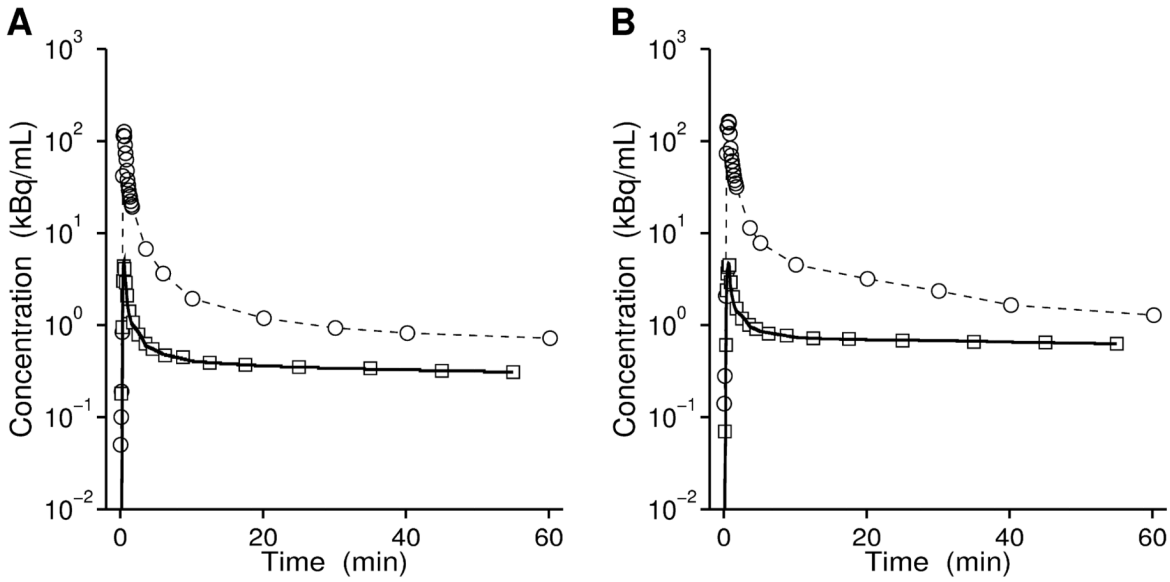

FIGURE 5.
Representative fits (bold solid lines) from 2T4K model using plasma input functions uncorrected for radiolabeled metabolites (open circles) for whole brain gray matter (open squares) for ^{11}C-tariquidar (A) and ^{11}C-elacridar (B).

Europe PMC Funders Author Manuscripts

Europe PMC Funders Author Manuscripts

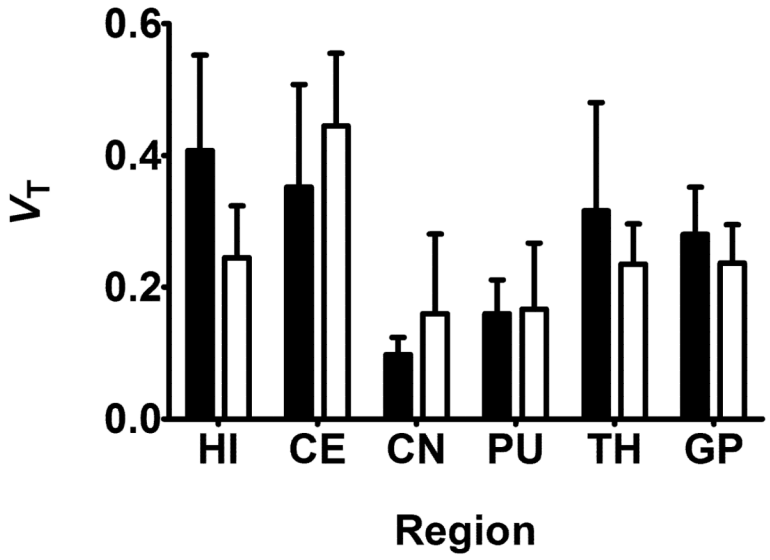

FIGURE 6.

Mean (+SD) 2T4K model-derived V_T values (using plasma input function uncorrected for radiolabeled metabolites) for ^{11}C-tariquidar (black bars, n = 5) and ^{11}C-elacridar (white bars, n = 4, subject 10 not included) in different brain regions. HI = hippocampus; CE = cerebellum; CN = caudate nucleus; PU = putamen; TH = thalamus; GP = gyrus precentralis.

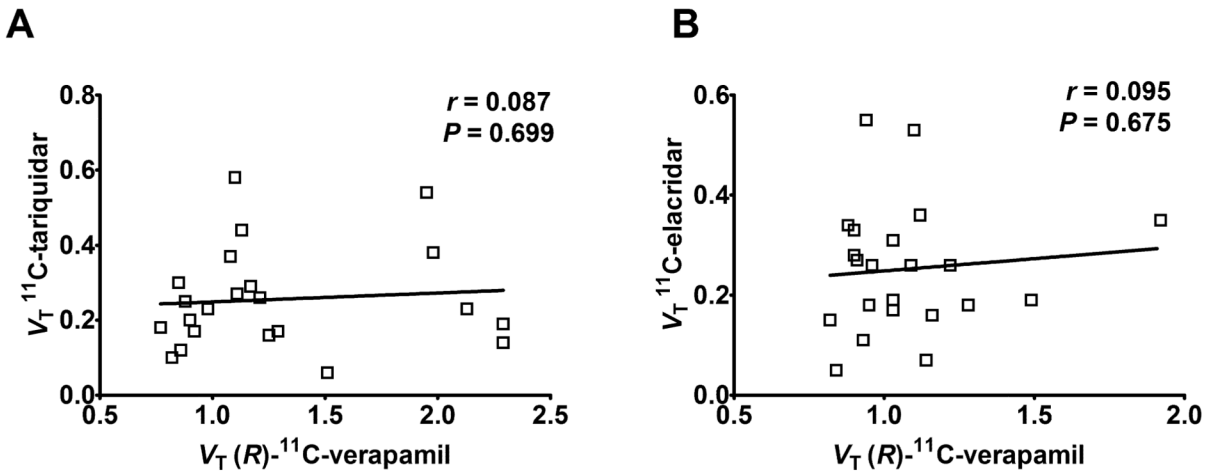

FIGURE 7.

Correlation of V_Ts of ^{11}C-tariquidar (A, n = 5) and ^{11}C-elacridar (B, n = 4, subject 10 not included) (using 2T4K model and plasma input function uncorrected for radiolabeled metabolites) with V_Ts of (R)-^{11} C-verapamil in hippocampus, cerebellum, caudate nucleus, putamen, thalamus and gyrus precentralis. Solid lines represent linear regression fits (r = Pearson correlation coefficient).

Europe PMC Funders Author Manuscripts

TABLE 1

Outcome Parameters for Whole Brain Gray Matter of the 1T2K and 2T4K Models * for ^{11}C-Tariquidar and ^{11}C-Elacridar

	1T2K		2T4K	
	^{11}C-tariquidar	**^{11}C-elacridar**	**^{11}C-tariquidar**	**^{11}C-elacridar**
K_1 (mL·mL^{-1}·min^{-1})	0.003±0.001 (0.002-0.004)	0.003±0.001 (0.002-0.003)	0.004±0.001 (0.003-0.004)	0.005±0.001 (0.004-0.005)
k_2 (min^{-1})	0.013±0.003 (0.010-0.016)	0.012±0.003 (0.009-0.014)	0.076±0.023 (0.055-0.097)	0.124±0.031 (0.094-0.155)
k_3 (min^{-1})			0.100±0.031 (0.073-0.127)	0.108±0.032 (0.076-0.140)
k_4 (min^{-1})			0.016±0.007 (0.010-0.022)	0.014±0.006 (0.007-0.020)
V_T (mL·mL^{-1})	0.23±0.04 (0.20-0.27)	0.24±0.09 (0.15-0.33)	0.35±0.07 (0.29-0.42)	0.36±0.07 (0.29-0.43)
V_b	0.050±0.008 (0.043-0.057)	0.046±0.003 (0.042-0.049)	0.046±0.006 (0.042-0.051)	0.042±0.003 (0.038-0.045)
AIC	−34.1±8.5	−33.8±7.7	−42.2±6.3	−49.7±1.9

Outcome parameters are given as mean ± SD (^{11}C-tariquidar: n = 5, ^{11}C-elacridar: n = 4, subject 10 excluded). In parentheses the 95% confidence intervals of the mean parameter estimates are given. K_1, k_2, k_3, k_4 : rate constants for exchange of radioactivity between plasma and brain compartments; V_T : distribution volume; V_b : blood volume fraction in brain; AIC: Akaike information criterion

* Data from 0-60 min was used and plasma input function was not corrected for radiolabeled metabolites.